A Theoretical Comparison of Self-Assembling α- and β-Peptide Nanostructures: Toward Design of β-Barrel Frameworks

Tamás Beke,[†] András Czajlik,[†] Balázs Bálint,[‡] András Perczel[†,‡,*]

[†]Protein Modelling Group MTA-ELTE, Institute of Chemistry, Eötvös Loránd University, P.O. Box 32, H-1538 Budapest, Hungary, and [‡]Laboratory of Structural Chemistry and Biology, Institute of Chemistry, Eötvös Loránd University, Pázmány Péter sétány 1/A, H-1117 Budapest, Hungary

ABSTRACT Self-assembling peptide-based nanotubes are among the most investigated bioactive compounds as a result of their numerous potential applications as novel biomaterials. To support rational bottom-up design of such artificial nanosystems, here we investigate structural and energetic properties of various sheet-derived nanotubes. We carried out high level quantum chemical calculations on large models, composed of up to 32 amino acids, and characterized structures from extended β-sheets to the molecular framework of β-barrel proteins. Surprisingly, enzyme-resistant nonnatural β-peptides have an affinity to form nanotubes that is remarkably higher than that of natural α-peptides. We analyzed the stability of both systems depending on (i) parallel or antiparallel orientation, (ii) the number of peptide strands, and (iii) the formed hydrogen bond pattern. Applicability is outlined by investigating guest molecules in the tubes. It is hoped that the structural and energetic data presented here will be effectively used in the design of novel peptide nanosystems.

KEYWORDS: peptide · nanotube · self-assembly · β-barrel · β-sheet · *ab initio* · DFT

Peptide nanotubes,[1–7] bioengineered transmembrane proteins (TMPs),[8] and peptide-based ion channels[9,10] are currently among the most investigated bioactive compounds. Their numerous potential applications include the rational development of antiviral[11] and antibacterial[12] therapeutics, liposome-mediated drug delivery,[13] and the design of novel biosensors.[14] In general, peptide nanotubes are composed of amino acids or amino acid derivatives, and the individual nanotubes self-assemble through hydrogen bonds or other noncovalent interactions (Figure 1). First representatives were built from cyclopeptides, which formed ordered nanostructures both in rod-shaped crystals obtained from aqueous media[4] and in lipid bilayers.[3] Although for the two environments the applied amino acid sequences in the cyclopeptides were totally different, the observed molecular framework was the same for both tubes. Theoretically, such a rigid tubular framework could be derived from the extended β-sheet, by forming a covalent bond between the N- and C-terminals of the peptide strands (Figure 1A). Alternatively, tubular structures could be derived from the same β-sheet by interconnecting the first and the last peptide strands through H-bonds. The obtained structures are closely related to a set of natural self-assembled macromolecues, the β-barrel proteins,[15,16] one major class of TMPs that carry out diverse functions in diverse organisms but are nevertheless unified by the common structural features of the molecular framework.[17] In general, they consist of 8–22 neighboring antiparallel β-strands that form a barrel structure. The fabrication of similar structures composed of linear self-assembling oligopeptides is highly desirable in bionanotechnology and in structural biochemistry.[18] The bottom-up design of such systems could be substantially advanced by using natural structures as a guide; however, characterizing atomic level structures and energetic properties of β-barrel frameworks is rather difficult using experimental techniques.[19] Additionally, natural or α-peptides have limited bioavailability owing to their low enzymatic resistance, and thus other sets of compounds should also be considered. As such, enzyme-resistant, nontoxic β-peptides[20] are ideal candidates for rational peptide-based design[21] (Figure 1B). Recently, on the basis of detailed quantum chemical (QC) structural analysis of β-amino acids[22,23] and β-peptides,[24] we showed that β-peptides spontaneously assemble into energetically stable nanotubes,[25] similarly as natural β-barrels do. Self-assembling potential of designed β-peptides was observed also

*Address correspondence to perczel@chem.elte.hu.

Received for review September 23, 2007 and accepted February 14, 2008.

Published online March 1, 2008.
10.1021/nn700252s CCC: $40.75

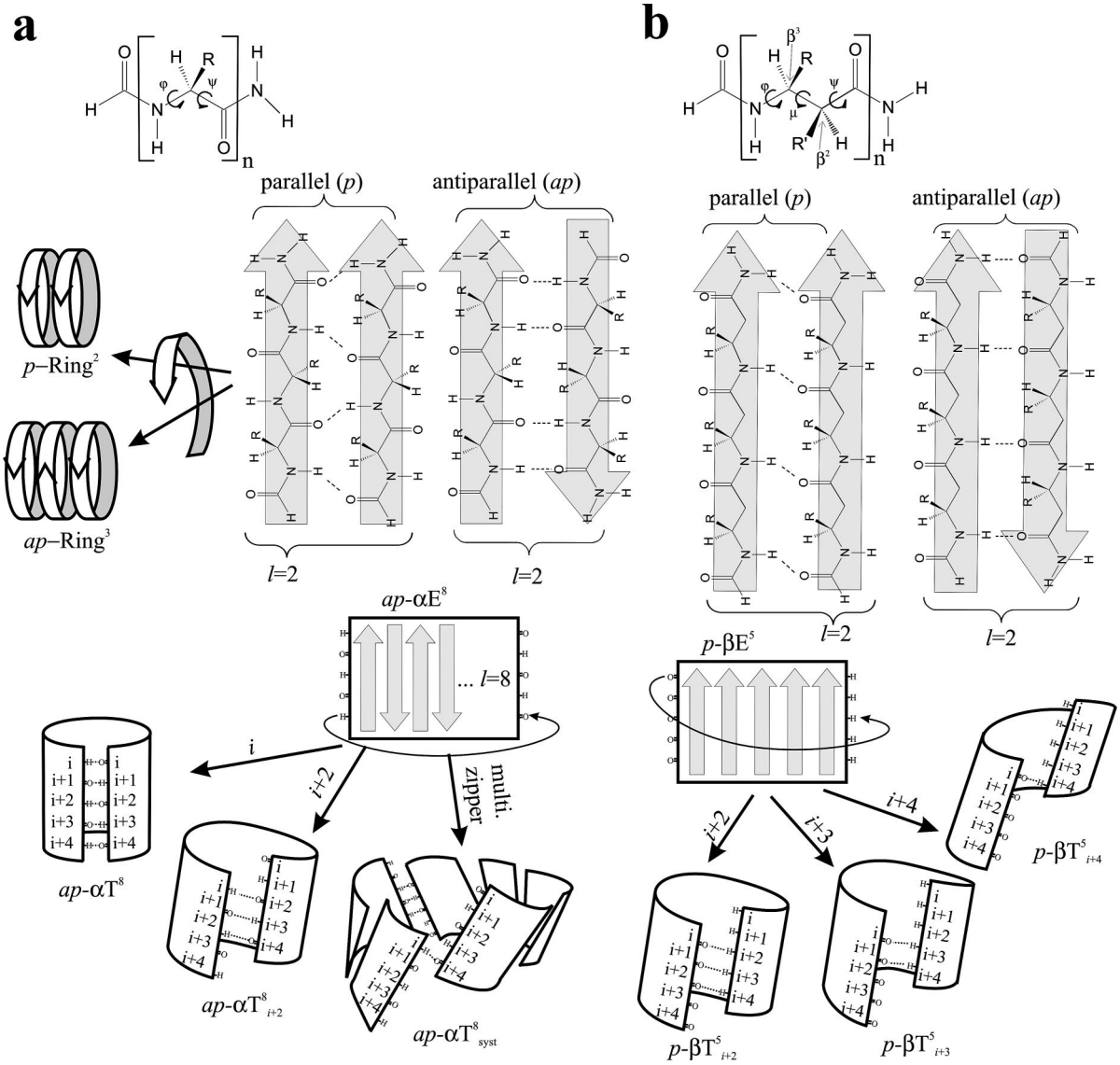

Figure 1. Schematic overview from monomers to investigated models of α- (a) and β-peptides (b). Common torsional angles of α- and β-amino acids (top), parallel and antiparallel arrangement of extended peptide strands (middle), and tubes composed of linear peptides (bottom), which can be formed by rolling up an extended sheet. In the present study, the systematically investigated molecular frameworks are composed of achiral amino acids, *i.e.*, R = R′ = H. (a) For α-peptides the orientation of side chains is alternating in one peptide strand. Parallel and antiparallel cyclo-peptide nanotubes can be derived from extended β-sheets (middle left). Tubes composed of linear peptides, which can be formed by rolling up an extended β-sheet (bottom): an untwisted tube with an $i \rightarrow (i)$ H-bond zipper, a twisted tube with a shifted $i \rightarrow (i + 2)$ zipper, and a fragment of a β-barrel protein with multiple shifted zippers. (b) For β-peptides the orientation of side chains is uniform in one peptide strand. Note that the extended sheets of β-peptides are not minimum energy structures.[25] Parallel tubes of β-peptide structures (bottom): twisted tubes interconnected by shifted $i \rightarrow (i + 2)$, $i \rightarrow (i + 3)$, and $i \rightarrow (i + 4)$ zippers, respectively. For details on nomenclature, see Applied Nomenclature in Methods.

by electronic circular dichroism and transmission electron microscopy.[26,27]

In this study, we report structural and energetic properties of three sets of model compounds, which were investigated by applied QC methods. First, theoretical calculations are validated on cyclo-peptide nanotubes. Second, multistranded linear α-peptide tubes are investigated from extended β-sheets to fragments cut out from a β-barrel protein, OmpA.[28,29] Third, energetic and structural properties of sheet-derived linear β-peptide tubes are described and compared to those of α-peptide nanotubes. Results show that linear β-peptides have an affinity to form sheet-derived nanotubes that is much higher than that of linear α-peptides. The intensive computational development of recent years made quantum mechanics and combined quantum mechanics/molecular mechanics (QM/MM) methods suitable to describe accurately structural and energetic properties of amino acids,[23,30,31] oligopeptide systems,[32–34] and oligo- and polypeptide nanosystems.[36–40]

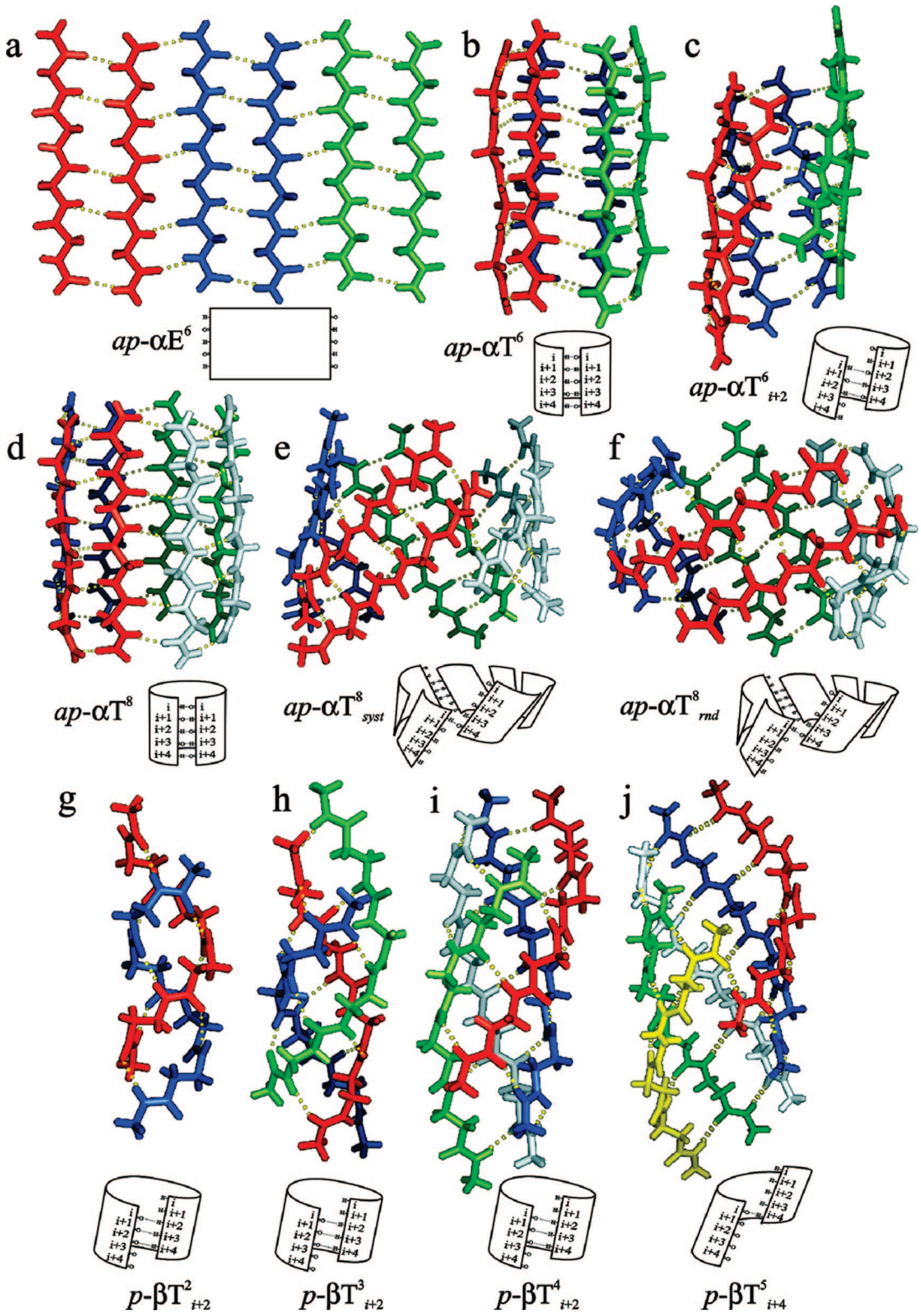

Figure 2. Selected structures of investigated α- and β-peptide models. (a−f) Antiparallel sheet-derived structures composed of 6 and 8 α-peptide strands, *ap*-[HCO-(α-Gly)$_4$-NH$_2$]$_{6/8}$. Neighboring peptide strands have the same color, and hydrogen bonds are labelled by dashed yellow lines. (a) The 6-stranded extended antiparallel α-peptide sheet, *ap*-αE^6. (b) The 6-stranded untwisted tube. (c) The 6-stranded tube with an $i \rightarrow (i + 2)$ zipper (*i.e.*, between the red and the green strands). (d) The 8-stranded untwisted tube. (e) The 8-stranded OmpA fragment having multiple $i \rightarrow (i + 2)$ zippers, except between the first (bright blue) and last (red) strands, which are connected by an $i + 4$ zipper. (f) The second OmpA fragment, *ap*-αT$^8_{rnd}$. This structure is elliptic, rather than a circular tube. (g−j) Parallel structures composed of 2−5 β-peptide strands, [CH$_3$CO-(β-Ala)$_4$-NHCH$_3$]$_l$ ($2 \leq l \leq 5$). Each tube has a shifted $i + 2$ H-bond zipper, except as noted otherwise. (g) The 2-stranded tube. (h) The 3-stranded tube. (i) The 4-stranded tube. (j) The 5-stranded parallel β-peptide tube, *p*-βT$^5_{i+4}$, with an $i + 4$ zipper operative between the first (yellow) and the last (red) strands. For nomenclature, see Methods.

TABLE 1. Selected Structural and Energetic Parameters of Investigated α-Peptide Systems, [HCO-(Gly)$_4$-NH$_2$]$_l$ ($4 \leq l \leq 8$), Obtained at the B3LYP/6-311++G(d,p)//RHF/3-21G Level of Theory; for Nomenclature, See Methods

structure	strand × res = unit[a]	D[b]	H-b[c]	$d_{O\cdots H}$[d]	ΔE[e]
ap-αE^4	4 × 4 = 16		15	1.90	0.0
p-αE^4			15	1.95	8.0
ap-αT^4		~5.9	20	2.16	9.8
p-αT^4		~5.9	16 (20)[f]	2.22	25.2
p-αE^5	5 × 4 = 20		20	1.91	0.0
p-αT^5		~7.0	21 (25)	2.08	13.9
ap-αE^6	6 × 4 = 24		25	1.89	0.0
p-αE^6			25	1.96	14.5
ap-αT^6		~8.6	30	1.99	−6.4
p-αT^6		~8.8	28 (30)	2.04	16.0
ap-αT$^6_{i+2}$		~9.2	28	1.96	2.9
p-αE^7	7 × 4 = 28		30	1.89	0.0
p-αT^7		~10.6	32 (35)	1.97	7.4
ap-αE^8	8 × 4 = 32		35	1.89	0.0
p-αE^8			35	1.88	7.8
ap-αT^8		~11.9	40	1.96	−15.5
p-αT^8		~11.9	40	1.97	11.8
ap-αT$^8_{rnd}$		18.8−14.2[g]	30[h]	1.90	23.0
ap-αT$^8_{syst}$		~15.5	30	1.90	25.6

[a]Strands × residues = units. [b]Average interior diameter in angstroms. [c]Number of hydrogen bonds. [d]Distance between O and H atoms in hydrogen bonds in angstroms. [e]Energies are in kcal · mol^{-1} and are relative to the energy of the corresponding antiparallel extended sheet structure. [f]For those structures where fewer hydrogen bonds are formed than the expected maximum, the maximum number is displayed in parenthesis. [g]Since *ap*-αT$^8_{rnd}$ is an elliptic tube, the highest and the lowest diameter is given. [h]As a result of amino protecting groups (-NH$_2$) at the C-terminal, three additional *cis* hydrogen bonds appear, which are not included.

TABLE 2. Selected Structural and Energetic Parameters of the Investigated β-Peptide Systems, [CH$_3$CO-(β-Ala)$_4$-NHCH$_3$]$_l$ ($2 \leq l \leq 5$), Obtained at the B3LYP/6-311++G(d,p)//B3LYP/6-31G(d) Level of Theory; for Nomenclature, See Methods

model	units[a]	D[b]	H-b[c]	$d_{O\cdots H}$[d]	ΔE[e]
p-βE^{2f}	2 × 4 = 8		5	2.10	0.0
p-βT$^2_{i+2}$		~4.5	8	2.02	−16.3
p-βE^3	3 × 4 = 12		10	2.00	0.0
p-βT$^3_{i+2}$		~6.0	13	1.95	−32.2
ap-βT$^3_{i+2}$		~5.6	13	2.03	−22.2
p-βE^4	4 × 4 = 16		15	1.94	0.0
p-βT$^4_{i+2}$		~6.9	18	1.93	−46.1
ap-βT$^4_{i+1}$		~6.7	19	2.01	−31.9
p-βE^5	5 × 4 = 20		20	1.98	0.0
p-βT$^5_{i+2}$		~8.8	23	1.93	−54.7
p-βT$^5_{i+3}$		~9.0	22	1.95	−45.1
p-βT$^5_{i+4}$		~10.3	21	1.97	−31.3

[a]Strands × residues = units. [b]Average interior diameter in angstroms. [c]Number of hydrogen bonds. [d]Distance between O and H atoms in hydrogen bonds. Values are in angstroms. [e]Energies are in kcal · mol^{-1} and are relative to the energy of the corresponding antiparallel extended sheet structure. [f]In the case of β-peptides the extended E structures were optimized with constraints that fix the model to be planar. Parameters of the 2- to 4-stranded parallel β-peptide systems were taken from ref 25.

RESULTS AND DISCUSSION

A Case Study: Cyclo-peptide Nanotubes. First designed cyclo-peptide nanotubes were composed of consecutive L- and D-amino acids such a way that all side chains were oriented toward the exterior matrix.[3,4] The individual cyclo-peptides or "rings" were interconnected through hydrogen bonds and according to experimental data the rings possessed antiparallel orientation.

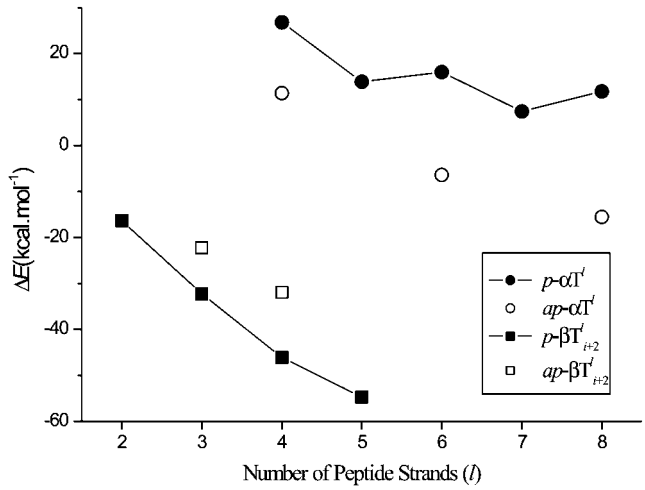

Figure 3. Relative energies (B3LYP/6-311++G(d,p)) of the most stable linear α- and β-peptide tubes as a function of the number of peptide strands. For each tube the energies are relative to the corresponding extended sheets (Tables 1 and 2). Tor α-peptide tubes, the antiparallel orientation and the $i \rightarrow i$ zippers are preferred, whereas for β-peptide tubes, the parallel orientation and the $i \rightarrow (i + 2)$ zippers are preferred. For nomenclature see Methods.

To validate applied QC methods to experimental data, we built up two sets of models from 1 to 4 cyclo-octapeptide rings, composed of achiral glycines (cyclo(G)$_8$) and chiral L- and D-alanines (cyclo(Aa)$_4$), respectively (Figure S1 and Table S1in Supporting Information). Energy profiles show that the self-assembly of the individual cyclo-peptides is favored by some 30 kcal · mol^{-1} for every newly added ring, for which the stabilization energy is roughly constant for both achiral and chiral model sets. Note that for the antiparallel structures an additional ~5 kcal · mol^{-1} stabilization energy is present with respect to the parallel rings. The observed average O···N distance in the hydrogen bonds of antiparallel structures (Table S1) is in full agreement with average values obtained experimentally by using FT-IR spectroscopic analysis (2.85 Å).[4] The preference of antiparallel structures observed for both model sets is also in consistence with previous experimental investigations.[3,4] The results suggest that the driving force of the self-assembly is the large energy gain due to the formation of hydrogen bonds between the rings. It is proposed that the observed structures are formed as a result of the stability of the molecular framework; however, to initiate this self-assembly the various other parameters, *e.g.* pH,[4] side chains, exterior matrix,[3] *etc.*, should be carefully adjusted to each other. The good correlation between experimental and theoretical data proposes that structural and energetic investigation of systems composed of 30+ amino acids can be effectively performed by QC

TABLE 3. Overview of Structural Properties of Linear α- and β-Peptide Tubes[a]

investigated property	α-peptides	β-peptides
smallest system capable of forming a nanotube	4-stranded, *ap*-βT^4	2-stranded, *p*-βT^4_{i+2}
preferred orientation	antiparallel	parallel
orientation of side chains	alternating	uniform
smallest system capable of having guest molecules or inner side chains	6-stranded	4-stranded
smallest nanotube, which is more stable than extended sheet	6-stranded, *ap*-βT^6, $\Delta E = -6.4$	2-stranded, *p*-βT^4_{i+2}, $\Delta E = -16.3$
most stable system investigated	*ap*-βT^8, $\Delta E = -15.5$	*p*-βT^5_{i+2}, $\Delta E = -54.7$
relative stability of the nanotubes correlates with the number of H-bonds	yes	no
average diameter of largest system investigated	15.5 Å (8-stranded with multiple zippers)	10.3 Å (5-stranded with a single $i \rightarrow (i + 4)$ zipper)

[a]Energies are in kcal · mol^{-1}.

calculations. For further details see Methods and Supporting Information.

Linear α-Peptide Tubes. Supposing an ideal case, nanotubes composed of linear α-peptides could be formed by simply rolling up a layer of β-sheet and by connecting the last and the first peptide strands through hydrogen bonds (Figure 1A). In this way one may obtain an untwisted tube with an "H-bond zipper" where the *i*th H-(N) forms a H-bond with the *i*th O═(C), the $(i + 1)$th H-(N) with the $(i + 1)$th O═(C), *etc*. This H-bond pattern, however, could be shifted. For instance, the *i*th H-(N) can form a hydrogen bond with the $(i + 2)$th *O*═(C), *etc*., called an $i \rightarrow (i + 2)$ zipper, which results in a twisted tube. Note that in the latter case only two peptide strands in the tubular structure are interconnected by an $i \rightarrow (i + 2)$ zipper, while the rest of the H-bonds form an $i \rightarrow (i)$ H-bond pattern. Further on, when applying multiple shifted zippers, the framework of β-barrel proteins is retained. Accordingly, extended β-sheet and tubular α-peptide models composed of 3–8 strands were built up and submitted to QC calculations (Figure 2). Note that, because of the alternating orientations of amide bonds, a fully antiparallel tube cannot be formed from an odd number of α-peptide strands.

In the case of the untwisted tubular assemblies with an $i \rightarrow (i)$ zipper, it is found that the 3-stranded tubes cannot be formed and even 4- and 5-stranded tubes are energetically less stable than the reference β-sheets (Table 1 and Figure 3). As the number of peptide strands increases to 6, an additional stabilization occurs and the tubular structure becomes slightly more stable than the extended reference structure. For the 8-stranded systems the antiparallel nanotube is the most stable structure investigated. The observed relative energy distribution is in line with the H-bond parameters that are unfavorable for the 4-stranded tubes but systematically improve as the number of strands increases (Table 1 and Table S2). For parallel structures, fewer H-bonds are found than the expected maximum even for sterically less crowded larger models such as the 7-stranded tube.

To compare energetic and structural parameters of the untwisted tubes to those with shifted $i \rightarrow (i + 2)$ or multiple H-bond zippers, an antiparallel 6-stranded α-peptide tube with a single $i \rightarrow (i + 2)$ type shift, *ap*-αT^6_{i+2}, (Figure 2C) and two fragments cut out from β-barrel protein OmpA,[28,29] *ap*-αT^8_{syst} (Figure 2E) and *ap*-αT^8_{rnd} (Figure 2F), were investigated. The 6-stranded tube, containing 28 H-bonds, is +9.3 kcal · mol^{-1} less stable compared to the untwisted tube, with 30 H-bonds (Table 1). This promotes a ~4.6 kcal · mol^{-1} stabilization energy difference per hydrogen bond. In the case of the 8-stranded models, the stabilization energy difference between the most stable untwisted tube, *ap*-αT^8, and the two OmpA fragments is again proportional to the number of H-bonds present in the structures: a ~4 kcal · mol^{-1} energy loss per H-bond can be observed (Table 1). Considering the effect of shifted H-bond zippers on the interior diameter (*D*), a single $i \rightarrow (i + 2)$ shifted zipper in *ap*-αT^6_{i+2} results an approximate 0.6 Å increase in *D* (Table 1), whereas the multiple zippers of *ap*-αT^8_{syst} and the elliptic *ap*-αT^8_{rnd} could increase the diameter by 3.5 and ~4.5Å, respectively.

In each case we found that parallel models were energetically less favorable compared to their antiparallel representatives, which is in agreement with previous results on sheet structures.[33] Additionally, parallel tubes composed of 4–7 strands form fewer H-bonds than the expected maximum, and even the large 8-stranded parallel tube is less stable than the reference β-sheets (Table 1). The preference of the antiparallel orientation is in agreement with the experimental results for β-barrels.[17,41] Surprisingly, in every case investigated, the corresponding untwisted tube is an energetically more preferred framework compared to the twisted tubes with shifted H-bond zipper(s). Thus, it is proposed that the main reason for the preference of multiple shifted zippers in β-barrel proteins is not the high stability of the formed backbone framework.

Linear β-Peptide Tubes Compared to Linear α-Peptide Tubes. Recently, we reported that extended parallel sheets of β-peptides were not stable according to theoretical calculations (Figure 1B).[25] Instead, these assemblies spontaneously formed tubes that were more stable than the sheet structures even for 2-stranded models. For 4-stranded tubes the stabilization energy became more than 40 kcal · mol^{-1} (Table 2). For every model set (*i.e.*, for models composed of the same number of peptide strands) the most stable structures had an $i \rightarrow (i + 2)$ zipper (in ref 25 they were called an $i + 3$ type pattern of H-bonds) (Figure 1B and Figure 2). Interestingly, as $i \rightarrow$ (i), $i \rightarrow (i + 1)$, and $i \rightarrow (i + 2)$ zippers were applied, the number of hydrogen bonds decreased; nevertheless, increasingly higher stabilization energies occurred (Table 2 in ref 25). This phenomenon was partially explained by the improving hydrogen bond parameters. Additionally, since the fully extended conformation, φ, μ, $\psi = 180°$, of one β-Ala monomer was found as a transition state structure rather than a minimum,[22] the reasons for tube formation could also originate from favorable changes in the backbone geometry of the monomeric units. Here, to compare the tubular molecular frameworks of the α-peptide and β-peptide systems, we extended our previous calculations to the 5-stranded parallel and to some of the antiparallel β-peptide tubes.

For the 5-stranded β-peptide systems, the stabilization energy of the tube with $i \rightarrow (i + 2)$ zipper relative to the extended sheet is 54.7 kcal · mol^{-1} (Table 2 and Table S3). When increasing the shift in the H-bond zipper to $i + 3$ and $i + 4$, the stabilization energy of the tubes decrease. Accordingly, for the 2- to 5-stranded parallel β-peptide systems the twisted tubes with $i \rightarrow (i + 2)$ H-bond zippers are the most stable.

Considering the antiparallel β-peptide tubes, the 2-stranded system cannot be found as a minimum energy structure. For the 3- and 4-stranded tubes with $i \rightarrow (i + 2)$ and $i \rightarrow (i + 1)$ zippers, respectively, a similar magnitude of stabilization can be observed as for parallel assemblies; however, the additional stability is smaller (Table 2 and Table S3). Accordingly, the antiparallel orientation is less favorable, which is also supported by the high deviation in the torsional angles.

When comparing the α- and β-peptide tubes (Table 3), it should be underlined that although pleated sheet is a common structural element of natural α-peptides, the similarly extended sheet-like structure of β-peptides is not found to be a minimum.[22,25,24] Thus, the affinity for forming sheet-derived tubes is much larger for β-peptides: the number required to form an energetically stable nanotube framework relative to the extended sheet structure is 6 for α-peptides (Table 1) but only 2 for β-peptides (Table 2 and Figure 3). When considering stability of the most stable tubes, the 8-stranded α-peptide tube has 15.5 kcal · mol^{-1} stabilization energy, whereas this value is 54.7 kcal · mol^{-1} for a 5-stranded β-peptide tube (Figure 3)! Further on, in the case of α-peptides the difference in relative stability between various tubes is proportional to the number of hydrogen bonds, whereas for β-peptides the increasingly twisted 3- and 4-stranded tubes show a considerable energy gain despite the decreasing number of H-bonds (Table 2 in ref 25). This is a rather uncommon phenomenon, which is currently not well understood; however, it could partially be explained by improved geometric and H-bond properties of the more twisted tubes. Considering the interior diameter, in the case of the 6-stranded antiparallel α-peptide tube, increasing the shift in the H-bond zipper from i to $i + 2$ enlarges D from ~8.6 to ~9.2 Å. In contrast, the similarly large shift from $i + 2$ to $i + 4$ for the 5-stranded β-peptide tubes enlarges D from ~8.8 to ~10.3 Å (Table 2), which matches the value of the 7-stranded untwisted α-peptide tubes. Putatively, in nanotubes fewer β- than α-peptide strands would be required to have a large enough interior diameter for various inner side chains.

Applicability. To test the effect of different side chains on the investigated tubular structures, selected systems with small chiral residues were submitted to QC calculations for both α- and β-peptides. Because of steric reasons, a 4-stranded tubular system, composed of only natural α-L-amino acids, cannot be formed (data not shown). Thus, we investigated a 4-stranded parallel model composed of HCO-(L-Ala-D-Ala)$_2$-NH$_2$ peptides, where all the side chains point toward the exterior matrix (Figure S2). Results on this model, *p*-[HCO-(L-Ala-D-Ala)$_2$-NH$_2$]$_4$, show that 4-stranded systems are sterically too tight for chiral α-peptides, since H-bonds are observed to form only at the terminals of the peptide strands. By increasing the number of strands to 6, the tubular structure could keep the H-bonds even with small inner side chains oriented toward each other (Figure S2). The positioning of the inner methyl side chains proposes that, similarly to other natural and artificial assemblies,[42] at a specific side chain composition, a similar system could be used to coordinate or encapsulate selected molecules.

For β-peptide nanotubes, the 4-stranded models already have a large enough interior diameter to incorporate compounds of various size and nature. Accordingly, water, acetonitrile, alkane chain, and potassium ions were inserted into parallel and antiparallel 4-stranded tubes (Figure S3). The QC results indicate that tubes both with polar and with apolar guest molecules inside are able to keep their initial fold. In contrast, many hydrogen bonds of the tube with the potassium ions break up, which shows that assemblies without interior polar side chains could not perform as effective ion channels. However, the quantum chemically accurate energetic description of ionic interactions in such large systems is beyond the scope of this study.

Finally, some general structural properties of α- and β-peptides should be considered: the orientation of side chains alternates for α-peptides, which results in one side chain pointing toward the exterior matrix while the consecutive one pointing toward the interior of the tube (Table 3). In contrast, the side chains of β-peptide tubes are directed uniformly. Additionally, a β-amino acid can be easily substituted on both β^2- and β^3-carbon atoms, resulting in one side chain pointing toward the inner axis and one toward the exterior matrix.[21] For α-peptide tubes, the antiparallel arrangement is a more favorable backbone framework, whereas for β-peptide tubes the parallel orientation is preferred.

It should be noted that, similarly as in the case of α-peptides, the applied side chains and the solvent have a great effect on the energetic preference of these structures; nevertheless, investigation of such additional parameters is beyond the scope of this study.

CONCLUSIONS

In this study, backbone frameworks of three different types of peptide nanotubes were investigated. Their structural and energetic parameters are described at the quantum chemical level. According to QC calculations, during self-assembly of cyclo-peptide models a significant stabilization energy occurs, which is explained by the formation of a preferred molecular framework. The structural parameters obtained are in agreement with the available experimental results.

Considering frameworks of linear peptide nanotubes, it is proposed that α-peptides have a moderate affinity to form β-sheet-derived tubes. In contrast, formation of β-peptide nanotubes is rather favorable relative to extended sheet structures. Nanotubes can readily be formed even from two β-peptide strands, and as the number of β-peptide strands increases to 5, the relative stability of a β-peptide nanotube becomes more than 50 kcal $\cdot$ mol^{-1} (Figure 3). In contrast to α-peptide systems, the high stabilization energies observed for β-peptide tubes do not correlate with the number of hydrogen bonds. The outlined tendencies are totally different from the ones observed for the α-peptide nanostructures (Table 3). Considering the uniform direction of side chains in these β-peptide tubes as well as the versatile set of mono- and disubstituted amino acids available,[21] it is expected that under suitable conditions these supersecondary structures have a great potential in both medicinal use and bioorganic nanoengineering. However, to characterize such peptide nanosystems in detail, further experimental and theoretical studies, which involve models with side chains and consider various solvents, are needed. Nevertheless, it is hoped that the accurate structural data presented on molecular frameworks of α- and β-peptide tubular nanosystems will be effectively applied in the design of novel functionalized nanotubes.

METHODS

Applied Nomenclature. For all systems the prefix "*p*" stands for parallel and "*ap*" stands for for antiparallel arrangement. For cyclo-peptide systems a simplified nomenclature is applied, based on the number of cyclo-peptides, "rings", appearing in the model (*e.g.*, *ap*-ring^3 stands for a cyclo-peptide system composed of three cyclo-peptides in antiparallel orientation). In general, for linear systems extended (E) sheet-like structures and tubular (T) structures are distinguished. Superscripts count the number of peptide strands within the model. In the parenthesis "α" labels natural- or α-peptides, and "β" stands for β-peptides, *e.g.* *p*-βT^3 is a parallel tubular structure, composed of three tetra-β-peptides. The twisted tubes are simply differentiated from the untwisted shapes by labeling the closing set of H-bonds or the "H-bond zippers", which interconnect the first and the last strand in the tube (Figure 1). An $i \rightarrow (i + 2)$ zipper reflects that the hydrogen bonds are operative between the *i*th H-bond donor or acceptor of the first and the $(i + 2)$th acceptor or donor of the last strand, *e.g.*, *ap*-αT^6_{i+2}. Note that natural β-barrel proteins usually have multiples of such shifted zippers, which here are simply referred to as "multiple zippers". For clarity, the more precise but complex shear numbers,[43] which are generally used to characterize the twist of β-barrels, are not used in this study.

Computational Details. ***Precision and Accuracy: Comparative Calculations To Validate the Optimal Level of Theory Applied.*** Earlier studies show that RHF/3-21G geometry optimizations supported by higher level single point calculations provide rather good energy for β-peptide systems,[22,24] *e.g.*, for small β-peptide models R^2 =0.99 between B3LYP/6-311++G(d,p)//RHF/3-21G and B3LYP/6-311++G(d,p) energies.[22] Similar conclusions on the good performance of RHF/3-21G geometries were drawn for models composed of α-amino acids.[44–46] While structure and conformational changes of large systems are in general investigated by molecular dynamics simulations, semiempirical methods can also be effectively used to obtain the geometry of large systems and submit it to single point energy calculations.[40] As a result of the recent computational development, in this study the investigated models are treated at the quantum mechanic level, using both *ab initio* and density functional theory calculations on large models composed of up to 320 atoms. Note that for such a large structure (*i.e.*, 1 bxw), even at the RHF/3-21G level of theory, 1800+ basis functions are required, which increases to 4700+ when larger basis sets are used (*i.e.*, at the B3LYP/6-311++G(d,p) level). Nevertheless, to validate RHF/3-21G geometries and to estimate the effect of basis set and electron correlation on the energetic and structural properties of the systems investigated, four pairs of peptide models, *p*-[CH_3CO-(β-Ala)$_4$-$NHCH_3$]$_l$ ($2 \leq l \leq 4$) (*i.e.*, *p*-βE^2, *p*-βT^2_{i+2};*p*-βE^3, *p*-βT^3_{i+2};*p*-βE^4, *p*-βT^4_{i+2}),[25] as well as *p*- and *ap*-[HCO-(Gly)$_4$-NH_2]$_4$ (*i.e.*, *p*-αT^4, *ap*-αT^4) composed of 104−208 atoms, were submitted to both RHF/3-21G and B3LYP/6-31G(d) level of theory calculations. Based on these eight structures, the average difference between a total of 280 torsional angles obtained at these two levels of theory is 8.3° (Tables S4−S6 in Supporting Information). Furthermore, when comparing parameters of 101 hydrogen bonds obtained at the two different levels of theory, the average difference between O$\cdots$H and O$\cdots$N distances and α_{O-H-N} angles is 0.04 Å, 0.07 Å, and 4.28°, respectively (Tables S2, S3, S7, and S8 in Supporting Information), and thus it is concluded that differences between RHF/3-21G and B3LYP/6-31G(d) geometries are not significant. Finally, relative energy differences for the eight pairs of tubular structures are less than 0.8 kcal $\cdot$ mol^{-1} between B3LYP/6-311++G(d,p)//RHF/3-21G and B3LYP/6-311++G(d,p)//B3LYP/6-31G(d) levels of theory, which is more than a magnitude smaller than the stabilization energies discussed in this study. Additionally, optimization of the *p*-βT^5_{i+4} structure of the pentatpeptide *p*-[CH_3CO-(β-

Ala)$_4$-NHCH$_3$]$_5$ was carried out at the B3LYP/6-31G(d) level of theory, using both "normal" and "loose" optimization convergence criteria,[47] which resulted in a negligible 0.002 kcal · mol^{-1} difference. Accordingly, the application of loose convergence criteria for the investigated 5-stranded β-peptide systems is much more cost-efficient. Finally, the magnitude of the basis set superposition error (BSSE) was previously investigated both for α- and β-peptides and was found to be as small as 0.5 kcal · mol^{-1} at the B3LYP/6-311++G(d,p) level of theory.[25,33] On the basis of the above considerations, the B3LYP/6-311++G(d,p)//RHF/3-21G level of theory was chosen to describe properties of α-peptide systems and B3LYP/6-311++G(d,p)//B3LYP/6-31G(d) level of theory calculations are presented for β-peptide systems throughout this study.

Model Selection and Computational Details. All computations were carried out in the gas phase, using the Gaussian 03 Software package.[47] PyMOL was used for all structure figures (www.pymol.org). To validate the results obtained on peptide nanotube systems, calculations were performed on cyclo-peptide nanotubes for both parallel and antiparallel systems. Two sets of models were built up from 1 to 4 cyclo-octapeptide rings, composed of achiral glycines (cyclo(G)$_8$) and chiral L- and D-alanines (cyclo(Aa)$_4$), respectively (Figure S1 and Table S1). These structures were fully optimized at the RHF/3-21G level of theory, followed by single point calculations at the B3LYP/6-311++G(d,p)//RHF/3-21G level of theory. For the systematic investigation of the linear peptide assemblies, every model was built from tetrapeptides containing only achiral amino acids (*e.g.*, glycine for α- and β-alanine for β-peptides). Investigated structures of linear α-peptide systems, composed of 4–8 parallel or antiparallel peptide strands (*p*- or *ap*-[HCO-(Gly)$_4$-NH$_2$]$_l$ ($4 \leq l \leq 8$)) were optimized at the RHF/3-21G level of theory, followed by single point calculations at the B3LYP/6-311++G(d,p)//RHF/3-21G level of theory. Additionally, two fragments composed of 8 tetrapeptide strands in antiparallel orientation were cut out from the X-ray structure of the OmpA β-barrel protein,[29,28] the side chains were removed, and the obtained framework structures (composed of 32 glycine residues) were submitted to full optimization at the RHF/3-21G level of theory, followed by B3LYP/6-311++G(d,p)//RHF/3-21G single point energy calculations. Both structures had multiple zippers. The first model, *ap*-αT^8_{rnd}, was cut out with as many hydrogen bonds between the consecutive peptide strands as possible (at least three) and thus contained only $i \rightarrow (i + 1)$ and $i \rightarrow (i + 2)$ zippers, but the overall H-bond pattern was random (Figure 2F). The second one, *ap*-$\alpha T_{syst}{}^8$, was cut out using a systematic hydrogen bond pattern, with alternating $i \rightarrow (i)$ and $i \rightarrow (i + 2)$ zippers, except between the first and eighth peptide strands, which had an $i \rightarrow (i + 4)$ zipper (Figures 1C left and 2E). To prevent the formation of "*cis* hydrogen bonds" due to the C-terminal amino protecting group (-NH$_2$), for the latter structure the N- and C-terminals were protected by acetyl (CH$_3$CO-) and *N*-methyl amino (-NH-CH$_3$) groups, respectively. Linear α-peptide tubes with chiral residues, *p*-[HCO-(L-Ala-D-Ala)$_2$-NH$_2$]$_4$ and {*p*-[HCO-(L-Ala-L-Ala-Gly-Gly)$_2$-NH$_2$]$_3$ *p*-[HCO-(Gly-Gly-L-Ala-L-Ala)$_2$-NH$_2$]$_3$} were submitted to full geometry optimization at the RHF/3-21G level of theory. The investigated tubular structures of simple β-peptide systems, *ap*-[CH$_3$CO-(β-Ala)$_4$-NHCH$_3$]$_l$ ($2 \leq l \leq 4$) as well as *p*-[CH$_3$CO-(β-Ala)$_4$-NHCH$_3$]$_5$ were fully optimized at the B3LYP/6-31G(d) level. In the case of the 5-stranded ($l = 5$) parallel β-peptide structures, optimizations were performed with "loose" convergence criteria.[47] The obtained structures were submitted to single point calculations at the B3LYP/6-311++G(d,p)//B3LYP/6-31G(d) level of theory. In the case of 5-stranded extended sheet structure, *p*-βE^5 torsional angle constraints were applied to keep the extended nature of the model. Models incorporating H$_2$O, CH$_3$CN, C$_{20}$H$_{42}$, or K$^+$ inside the tubes were fully optimized at the RHF/3-21G level of theory. Cartesian coordinates of the models investigated are available on request; please contact the corresponding author.

Acknowledgment. This research was supported by grants from the Hungarian Scientific Research Foundation (OTKA T046994 and TS044730), MediChem2, and ICGEB Hun04-03. The ELTE computer facility and the HPC group, U. Szeged were used for several computations. The authors would like to thank Ö. Farkas for helpful discussions.

Supporting Information Available: This material includes additional discussion, figures, and tables on cyclo-peptide nanotubes, extended tables on the structural and energetic properties of the linear peptide structures investigated, and figures on the structures with guest molecules and side chains inside the tubes. This information is available free of charge *via* the Internet at http://pubs.acs.org.

REFERENCES AND NOTES

1. Reches, M.; Gazit, E. Controlled Patterning of Aligned Self-Assembled Peptide Nanotubes. *Nat. Nanotechnol.* **2006**, *1*, 195–200.
2. Zhang, S. Fabrication of Novel Biomaterials through Molecular Self-Assembly. *Nat. Biotechnol.* **2003**, *21*, 1171–1178.
3. Ghadiri, M. R.; Granja, J. R.; Buehler, L. K. Artificial Transmembrane Ion Channels from Self-Assembling Peptide Nanotubes. *Nature* **1994**, *369*, 301–304.
4. Ghadiri, M. R.; Granja, J. R.; Milligan, R. A.; McRee, D. E.; Khazanovich, N. Self-Assembling Organic Nanotubes Based on a Cyclic Peptide Architecture. *Nature* **1993**, *366*, 324–327.
5. Görbitz, C. H. The Structure of Nanotubes Formed by Diphenylalanine, the Core Recognition Motif of Alzheimer's β-Amyloid Polypeptide. *Chem. Commun. (Cambridge)* **2006**, *2332*, 2334.
6. Reches, M.; Gazit, E. Casting Metal Nanowires within Discrete Self-Assembled Peptide Nanotubes. *Science* **2003**, *300*, 625–627.
7. Percec, V.; Dulcey, A. E.; Peterca, M.; Adelman, P.; Samant, R.; Balagurusamy, V. S.; Heiney, P. A. Helical Pores Self-Assembled from Homochiral Dendritic Dipeptides Based on L-Tyr and Nonpolar α-Amino Acids. *J. Am. Chem. Soc.* **2007**, *129*, 5992–6002.
8. Silverman, J. A.; Balakrishnan, R.; Harbury, P. B. Reverse Engineering the (β/α)8 Barrel Fold. *Proc. Natl. Acad. Sci. U.S.A.* **2001**, *98*, 3092–3097.
9. Fyles, T. M. Synthetic Ion Channels in Bilayer Membranes. *Chem. Soc. Rev.* **2007**, *36*, 335–347.
10. Gokel, G. W.; Carasel, I. A. Biologically Active, Synthetic Ion Transporters. *Chem. Soc. Rev.* **2007**, *36*, 378–389.
11. Horne, W. S.; Wiethoff, C. M.; Cui, C.; Wilcoxen, K. M.; Amorin, M.; Ghadiri, M. R.; Nemerow, G. R. Antiviral Cyclic D,L- α-Peptides: Targeting a General Biochemical Pathway in Virus Infections. *Bioorg. Med. Chem.* **2005**, *13*, 5145–5153.
12. Fernandez-Lopez, S.; Kim, H. S.; Choi, E. C.; Delgado, M.; Granja, J. R.; Khasanov, A.; Kraehenbuehl, K.; Long, G.; Weinberger, D. A.; Wilcoxen, K. M.; Ghadiri, M. R. Antibacterial Agents Based on the Cyclic D,L-α-Peptide Architecture. *Nature* **2001**, *412*, 452–455.
13. Popot, J. L.; Saraste, M. Engineering Membrane Proteins. *Curr. Opin. Biotechnol.* **1995**, *6*, 394–402.
14. Dietrich, C.; Schmitt, L.; Tampe, R. Molecular Organization of Histidine-Tagged Biomolecules at Self-Assembled Lipid Interfaces Using a Novel Class of Chelator Lipids. *Proc. Natl. Acad. Sci. U.S.A.* **1995**, *92*, 9014–9018.
15. Kleinschmidt, J. H. Membrane Protein Folding on the Example of Outer Membrane Protein A of *Escherichia coli*. *Cell. Mol. Life Sci.* **2003**, *60*, 1547–1558.
16. Wimley, W. C. The Versatile β-Barrel Membrane Protein. *Curr. Opin. Struct. Biol.* **2003**, *13*, 404–411.
17. Wimley, W. C. Toward Genomic Identification of β-Barrel Membrane Proteins: Composition and Architecture of Known Structures. *Protein Sci.* **2002**, *11*, 301–312.
18. Rausch, J. M.; Marks, J. R.; Wimley, W. C. Rational Combinatorial Design of Pore-Forming β-Sheet Peptides. *Proc. Natl. Acad. Sci. U.S.A.* **2005**, *102*, 10511–10515.
19. Lacapére, J.-J.; Pebay-Peyroula, E.; Neumann, J.-M.; Etchebest, C. Determining Membrane Protein Structures: Still a Challenge! *Trends Biochem. Sci.* **2007**, *32*, 259–269.

20. Nielsen, P. E. *Pseudo-Peptides in Drug Discovery*; Wiley-VCH: Weinheim, 2004; pp 33–113..
21. Seebach, D.; Beck, A. K.; Bierbaum, D. J. The World of β- and γ-Peptides Comprised of Homologated Proteinogenic Amino Acids and Other Components. *Chem. Biodiversity* **2004**, *1*, 1111–1239.
22. Beke, T.; Csizmadia, I. G.; Perczel, A. On the Flexibility of β-Peptides. *J. Comput. Chem.* **2004**, *25*, 285–307.
23. Möhle, K.; Günther, R.; Thormann, M.; Sewald, N.; Hofmann, H. J. Basic Conformers in β-Peptides. *Biopolymers* **1999**, *50*, 167–184.
24. Beke, T.; Somlai, C.; Perczel, A. Toward a Rational Design of β-Peptide Structures. *J. Comput. Chem.* **2006**, *27*, 20–38.
25. Beke, T.; Csizmadia, I. G.; Perczel, A. Theoretical Study on Tertiary Structural Elements of β-Peptides: Nanotubes Formed From Parallel-Sheet-Derived Assemblies of β-Peptides. *J. Am. Chem. Soc.* **2006**, *128*, 5158–5167.
26. Martinek, T. A.; Mándity, I. M.; Fülöp, L.; Tóth, G. K.; Vass, E.; Hollósi, M.; Forró, E.; Fülöp, F. Effects on the Secondary Structure and Self-Assembly of β-Peptides. *J. Am. Chem. Soc.* **2006**, *128*, 13539–13544.
27. Martinek, T. A.; Hetényi, A.; Fülöp, L.; Mandity, I. M.; Tóth, G. K.; Dékány, I.; Fülöp, F. Secondary Structure Dependent Self-Assembly of β-Peptides Into Nanosized Fibrils and Membranes. *Angew. Chem., Int. Ed.* **2006**, *45*, 2396–2400.
28. Pautsch, A.; Schulz, G. E. Structure of the Outer Membrane Protein A Transmembrane Domain. *Nat. Struct. Biol.* **1998**, *5*, 1013–1017.
29. Pautsch, A.; Schulz, G. E. High-Resolution Structure of the OmpA Membrane Domain. *J. Mol. Biol.* **2000**, *298*, 273–282.
30. Perczel, A.; Ángyán, J. G.; Kajtár, M.; Viviani, W.; Rivail, J. L.; Marcoccia, J. F.; Csizmadia, I. G. Peptide Models 1. Topology of Selected Peptide Conformational Potential-Energy Surfaces (Glycine and Alanine Derivatives). *J. Am. Chem. Soc.* **1991**, *113*, 6256–6265.
31. Head-Gordon, T.; Head-Gordon, M.; Frisch, M. J.; Brooks, C. L.; Pople, J. A. Theoretical Study of Blocked Glycine and Alanine Peptide Analogues. *J. Am. Chem. Soc.* **1991**, *113*, 5989–5997.
32. Zhao, Y. L.; Wu, Y. D. A Theoretical Study of β-Sheet Models: Is the Formation of Hydrogen-Bond Networks Cooperative? *J. Am. Chem. Soc.* **2002**, *124*, 1570–1571.
33. Perczel, A.; Gáspári, Z.; Csizmadia, I. G. Structure and Stability of β-Pleated Sheets. *J. Comput. Chem.* **2005**, *26*, 1155–1168.
34. Kubelka, J.; Keiderling, T. A. Differentiation of β-Sheet-Forming Structures: Ab Initio-Based Simulations of IR Absorption and Vibrational CD for Model Peptide and Protein β-Sheets. *J. Am. Chem. Soc.* **2001**, *123*, 12048–12058.
35. Beachy, M. D.; Chasman, D.; Murphy, R. B.; Halgren, T. A.; Friesner, R. A. Accurate Ab Initio Quantum Chemical Determination of the Relative Energetics of Peptide Conformation and Assessment of Empirical Force Fields. *J. Am. Chem. Soc.* **1997**, *119*, 5908–5920.
36. Beke, T.; Czajlik, A.; Csizmadia, I. G.; Perczel, A. Determining Suitable Lego-Structures to Estimate Stability of Larger Peptide Nanostructures Using Computational Methods. *Phys. Biol.* **2006**, *3*, S26–S39.
37. Pohl, G.; Beke, T.; Borbély, J.; Perczel, A. Prediction of Folding Preference of 10 kDa Silk-Like Proteins Using a Lego Approach and Ab Initio Calculations. *J. Am. Chem. Soc.* **2006**, *128*, 14548–14559.
38. Schatz, G. C. Using Theory and Computation to Model Nanoscale Properties. *Proc. Natl. Acad. Sci. U.S.A.* **2007**, *104*, 6885–6892.
39. Moran, A.; Mukamel, S. The Origin of Vibrational Mode Couplings in Various Secondary Structural Motifs of Polypeptides. *Proc. Natl. Acad. Sci. U.S.A.* **2004**, *101*, 506–510.
40. Qu, W.; Tan, H.; Chen, G.; Liu, R. Theoretical Studies of a Novel Photo-Switchable Self-Organized Peptide System. *Phys. Chem. Chem. Phys.* **2003**, *5*, 2327–2332.
41. Schulz, G. E. β-Barrel Membrane Proteins. *Curr. Opin. Struct. Biol.* **2000**, *10*, 443–447.
42. Kang, J.; Rebek, J., Jr. Acceleration of a Diels-Alder Reaction by a Self-Assembled Molecular Capsule. *Nature* **1997**, *385*, 50–52.
43. Liu, W.-M. Shear Numbers of Protein β-Barrels: Definition Refinements and Statistics. *J. Mol. Biol.* **1998**, *275*, 541–545.
44. Koo, J. C. P.; Lam, J. S. W.; Salpietro, S. J.; Chass, G. A.; Enriz, R. D.; Torday, L. L.; Varró, A.; Papp, J. G. How Reliable Could Economic Hartree-Fock Computations Be in Studying Large, Folded Peptides? A Comparative HF and DFT Case Study on N- and C-Protected Aspartic Acid. *J. Mol. Struct. (THEOCHEM)* **2002**, *619*, 143–194.
45. Möhle, K.; Hofmann, H. J. Stability Order of Basic Peptide Conformation Reflected by Density Functional Theory. *J. Mol. Model.* **1998**, *4*, 53–60.
46. Sahai, M. A.; Kehoe, T. A.; Koo, J. C.; Setiadi, D. H.; Chass, G. A.; Viskolcz, B.; Penke, B.; Pai, E. F.; Csizmadia, I. G. First Principle Computational Study on the Full Conformational Space of L-Proline Diamides. *J. Phys. Chem. A* **2005**, *109*, 2660–2679.
47. Frisch, M. J. *et al*. *Gaussian 03*, Revision 0.02; Gaussian, Inc.: Wallingford, CT, 2004.